

STANDARD MODEL PHYSICS AT LEP

S. BETHKE
 Max-Planck-Institut für Physik
 (Werner-Heisenberg-Institut)
 80805 München, Germany

Abstract. Selected topics on precision tests of the Standard Model of the Electroweak and the Strong Interaction at the LEP e^+e^- collider are presented, including an update of the world summary of measurements of α_s , representing the state of knowledge of summer 1999. This write-up of lecture notes¹ consists of a reproduction of slides, pictures and tables, supplemented by a short descriptive text and a list of relevant references.

1. Introduction

The physics of elementary particles and forces determined the development of the early universe and thus, of the structure of our world today (Fig. 1). According to our present knowledge, three families of quarks and leptons, four fundamental interactions, their respective exchange bosons and a yet-to-discover mechanism to generate particle masses are the ingredients (Fig. 2) which are necessary to describe our universe, both at cosmic as well as at microscopic scales.

Three of the four forces are relevant for particle physics at small distances: the Strong, the Electromagnetic and the Weak Force. They are described by quantum field theories, Quantum Chromodynamics (QCD) for the Strong, Quantum Electrodynamics (QED) for the Electromagnetic and the so-called Standard Model of the unified Electro-Weak Interactions [1]. The weakest force of the four, gravitation, is the major player only at large distances where the other three are, in general, not relevant anymore: the Strong and the Weak Force are short-ranged and thus limited to sub-nuclear distances, the Electromagnetic force only acts between objects whose net electric charge is different from zero.

¹Lecture given at the International Summer School "Particle Production Spanning MeV and TeV Energies", Nijmegen (The Netherlands), August 8-20, 1999.

Of the objects listed in Fig. 2, only the ν -neutrino (ν), the Graviton and the Higgs-boson are not explicitly detected to-date. Besides these particular points of ignorance, the overall picture of elementary particles and forces was completed and tested with remarkable precision and success during the past few years, and the data from the LEP electron-positron collider belong to the major important ingredients in this field.

This lecture reviews selected aspects of Standard Model physics at LEP. The frame of this write-up is not a standard and text-book-like presentation, but rather a collection and reproduction of slides, pictures and tables, similar as presented in the lecture itself. Since most of the slides are self-explanatory, the collection is only accompanied by a short, connecting text, plus a selection of references where the reader can find more detailed information.

2. LEP: machine, detectors and physics

A decade of successful operation of the Large Electron Positron collider, LEP [2] (Fig. 3), provided a wealth of precision data (Fig. 4) on the electroweak and on the strong interactions, through a multitude of e^+e^- annihilation final states (depicted in Fig. 5) which are recorded by four multi-purpose detectors, ALEPH [3], DELPHI [4], L3 [5] and OPAL [6].

In the phase which is called "LEP-I", from 1989 to 1995, the four LEP experiments have collected a total of about 17 million events in which an electron and a positron annihilate into a Z^0 which subsequently decays into a fermion-antifermion-pair (see Figs. 4 and 5). Since 1995, the LEP collider operates at energies above the Z^0 resonance, $\sqrt{s} = E_{cm} > M_{Z^0} \approx 91.1876 \text{ GeV}$ ("LEP-II"), up to currently more than 200 GeV in the centre of mass system. The different final states of e^+e^- annihilations can be measured and identified with large efficiency and confidence, due to the hermetic and redundant detector technologies realised by all four experiments.

An example of a hadronic 3-jet event, originating from the process $e^+e^- \rightarrow Z^0 \rightarrow q\bar{q}g$ with subsequent fragmentation of quarks and gluons into hadrons, as recorded by the OPAL detector (Fig. 6) [6], is reproduced in Fig. 7.

3. Precision tests of the Electroweak Interaction

The basic predictions of the Standard Model of Electroweak Interactions, for fermion-antifermion production of e^+e^- annihilations around the Z^0 resonance, are summarised in Fig. 8 to Fig. 11, see [1] and recent experimental reviews [7, 8, 9] for more details. Cross sections of these processes are energy (\sqrt{s} -) dependent and contain a term from Z^0 exchange, another from photon exchange as well as a γ - Z^0 interference term (Fig. 8).

Measurements of s -dependent cross sections around the Z^0 resonance provide model independent results for the mass of the Z^0 , M_{Z^0} , of the Z^0 total and partial decay widths, Γ_Z and Γ_f , and of the fermion pole cross sections, σ_f^0 .

Beyond the lowest order "Born Approximation", photonic and non-photonic radiative corrections must be considered (Fig. 9); the latter can be absorbed into "running coupling constants" (Fig. 10) which, if inserted into the Born Approximation, make the experimental observables depend on the masses of the top quark and of the Higgs Boson, M_t and M_H . Measurements of the fermion final state cross sections as well as of other observables like differential cross sections, forward-backward asymmetries and final state polarisations of leptons (Fig. 11) allow to extract the basic electroweak parameters.

Combined analyses of the data of all 4 LEP experiments by the "LEP Electroweak Working Group" [10] provide very precise results (Fig. 12): for instance, due to the precise energy calibration of LEP [11], M_{Z^0} is determined to an accuracy of 23 parts-per-million, and the number of light neutrino generations (and thus, of quark- and lepton-generations in general) is determined to be compatible with 3 within about 1% accuracy. From radiative corrections and a combination of data from LEP-I and LEP-II, M_t , M_H , the coupling strength of the Strong Interactions, α_s , the effective weak mixing angle $\sin^2 \theta_{\text{lept}}^{\text{eff}}$ and the Mass of the W -boson, M_W , can be determined with remarkable accuracy (except for M_H which only enters logarithmically). A list of the most recent results [9] is given in Fig. 13, where also the deviations of the experimental tests from the theoretical expectations are given by the number of standard deviations ("Pull").

Graphical representations of some of these results are given in Fig. 14 to Fig. 18. The significance of counting the number of light neutrino families, N_ν , from the measurement of the Z^0 line shape, based on ALEPH data from the 1990 and 1991 scan period, is displayed in Fig. 14. The gain in precision of electroweak parameters between 1987, before the era of LEP, and the LEP results of 1999 is demonstrated in Fig. 15, for the values of the leptonic axial and vector couplings, g_a and g_v .

The best result of the Higgs mass, M_H , is given in Fig. 16, calculated using two different input values for the uncertainty of the hadronic part of the running QED coupling constant, α_{had} [12, 13], together with the exclusion limit from direct Higgs production searches, $M_H > 95.2 \text{ GeV}$ (95% confidence level) [9].

The measured cross section for W pair production, $e^+e^- \rightarrow W^+W^-$ (σ_{WW}), is presented in Fig. 17, together with the Standard Model prediction and two "toy models" which demonstrate the importance of the ZWW triple gauge boson vertex and the e exchange diagram, see Fig. 5. A summary of

the available measurements (top) and indirect determinations, i.e. through radiative corrections (bottom), of the W mass is given in Fig. 18. More results and graphs are available from [9] and from the home page of the LEP Electroweak Working Group [10].

4. Jet Physics and Tests of QCD

A short introduction to the development of hadron physics, from the discovery of the neutron to the development of QCD and the experimental manifestation of gluons, is given in Fig. 19. The basic properties of QCD – in comparison with QED – are summarised in Fig. 20. The energy dependence of the strong coupling strength α_s , given by the so-called β -function in terms of the renormalisation scale μ and the QCD group structure parameters C_F, N_c, C_A and N_f , is described in Fig. 21.

In Fig. 22, the anatomy of the process $e^+e^- \rightarrow$ hadrons is illustrated. Factorisation is assumed to hold when splitting this process into an electroweak part (annihilation of e^+e^- into a virtual photon or Z^0 and subsequent decay into a quark-antiquark pair), the development of a parton (i.e. quark and gluon) shower described by perturbative QCD, a hadronisation phase which can be modelled using various different fragmentation or hadronisation models, and finally a parametrisation of the decays of unstable hadrons (according to measured decay modes and branching fractions) [14, 15, 16].

A list of the most prominent QCD topics covered by the LEP experiments is given in Fig. 23. For a more detailed introduction to QCD and hadronic physics at high energy particle colliders see e.g. [17]; earlier reviews of QCD tests at LEP can be found in [18, 19, 20].

One of the most prominent QCD-related measurements at LEP is the determination of α_s from the radiative corrections to the hadronic partial decay width of the Z^0 , which is summarised in Fig. 24. The ratio $R_Z = \Gamma_{\text{had}}/\Gamma_{\text{lept}}$ is a totally inclusive quantity which is independent of hadronisation effects, and QCD corrections are available in complete $\mathcal{O}(\alpha_s^3)$, i.e. in next-to-next-to-leading order QCD perturbation theory [21, 22]. The determination of α_s from R_Z , however, crucially depends on the validity of the predictions of the Electroweak Standard Model.

The basic principles of the physics of hadrons jets, which are interpreted as the footprints of energetic quarks and gluons, and the definition of hadron jets are described in Fig. 25. The most commonly used jet algorithms in e^+e^- annihilations are clustering procedures as first introduced by the JADE collaboration [23], and variants of this algorithm [24, 25, 26, 27] as listed in Tab. 1.

For these algorithms, relative production rates of n -jet events ($n =$

2, 3, 4, ...) are predicted by QCD perturbation theory, and are therefore well suited to determine α_s and to prove the energy dependence of α_s , see Fig. 26. In particular, the relative rate of 3-jet events, R_3 , is predicted to be proportional to α_s , in leading order perturbation theory. Corrections in complete next-to-leading order, i.e. in $O(\alpha_s^2)$, are available for these algorithms [25, 26].

Hadronisation effects, however, may significantly influence the reconstruction of jets. This can be seen in Fig. 27, where jet production rates are analysed using QCD model (Jetset) events of e^+e^- annihilation at $\sqrt{s} = 91.2$ GeV before and after hadronisation, i.e. at parton- and at hadron-level. The purity of 3-jet reconstruction, i.e. the number of events which are classified as 3-jet both on parton- and at hadron-level, normalised by the number of events classified as 3-jet on hadron level, is displayed in Fig. 28. The energy dependence of hadronisation corrections to measurements of 3-jet event production rates at fixed jet resolution y_{cut} is analysed in Fig. 29. From these studies, the original JADE and the Durham schemes emerge as the most "reliable" algorithms to test QCD in jet production from e^+e^- annihilations (for a comparative study of the newer Cambridge algorithm, see e.g. [28]).

Especially the JADE algorithm exhibits small and almost energy independent hadronisation corrections. This allows to test the energy dependence of α_s and thus, of asymptotic freedom, without actually having to determine numerical values of α_s , see Fig. 30 [29].

Hadronic event shapes (Fig. 31) are a common tool to study aspects of QCD, and in particular, to determine α_s . For many of these observables, QCD predictions in next-to-leading order ($O(\alpha_s^2)$) are available [25], and for some of them, the leading and next-to-leading logarithms were resummed to all orders [30].

The results of one such study, performed by L3 [31] using event shapes of LEP-I and LEP-II data plus radiative events at reduced centre of mass energies, is shown in Fig. 32, demonstrating the running of α_s . For more details on the determination of α_s from hadronic event shape and jet related observables, see e.g. [17, 18, 19, 32].

A list of high energy particle processes and observables from which significant determinations of α_s are obtained is given in Fig. 33. The most recent measurements, as an update to the world summary of α_s from 1998 [33], are listed in Fig. 34.

Table 2 summarises the current status of α_s results. The corresponding values of $\alpha_s(Q^2)$, where Q is the typical hard scattering energy scale of the process which was analysed, are displayed in Fig. 35. The data, spanning energy scales from below 1 GeV up to several hundreds of GeV, significantly

demonstrate the energy dependence of α_s , which is in good agreement with the QCD prediction.

Evolving these values of $\alpha_s(Q)$ to a common energy scale, $Q = M_{Z^0}$, using the QCD β -function in $O(\alpha_s^4)$ with 3-loop matching at the heavy quark pole masses $M_b = 4.7 \text{ GeV}$ and $M_c = 1.5 \text{ GeV}$ [34], results in Fig. 36, demonstrating the good agreement between all measurements. From the results based on QCD calculations which are complete to next-to-next-to-leading order (filled symbols in Fig. 36; see also Table 2), a new world average of

$$\alpha_s(M_{Z^0}) = 0.119 \pm 0.003 \quad [\text{in NNLO}]$$

is determined. The overall error is calculated using a method [35] which introduces a common correlation factor between the errors of the individual results such that the overall χ^2 amounts to 1 per degree of freedom. The size of the resulting overall uncertainty depends on the method and philosophy used to determine the world average of $\alpha_s(M_{Z^0})$, see [33] for further discussion.

References

1. see textbooks on Gauge Theories and Particle Physics, as for instance:
E. Leader, E. Predazzi, *An Introduction to Gauge Theories and Modern Particle Physics*, Vols. 1 and 2, Cambridge University Press, 1996;
C. Quigg, *Gauge Theories of the Strong, Weak and Electromagnetic Interactions*, Benjamin/Cummings (1983).
2. S. Myers, E. Picasso, *Contemp. Phys.* 31 (1990) 387.
3. ALEPH Collaboration, D. Buskulic et al., *Nucl. Inst. Meth. A* 360 (1995) 481.
4. DELPHI Collaboration, P. Abreu et al., *Nucl. Instr. Meth. A* 378 (1996) 57.
5. L3 Collaboration, O. Adriani et al., *Phys. Rep.* (1993) 236.
6. OPAL Collaboration, K. Ahm et al., *Nucl. Inst. Meth. A* 305 (1991) 275.
7. H. Burkhardt, J. Steinberger, *Ann. Rev. Nucl. Part. Sci.* 41 (1991) 55.
8. G. Quast, *Prog. Nucl. Part. Phys.* 43 (1999) 87.
9. J. M. Nich, *proc. of EPS-HEP '99, Tampere, Finland, July 1999*; CERN-EP/99-43.
10. The LEP Electroweak Working Group, CERN-EP/99-15;
<http://www.cern.ch/LEPEWWG/>.
11. R. Assmann et al., *Eur. Phys. J. C* 6 (1999) 187;
A. Blondel et al., *hep-ex/9901002*, submitted to *Eur. Phys. J. C*.
12. S. Eidelmann and F. Jegerlehner, *Z. Phys. C* 67 (1995) 585.
13. M. Davier and A. Hocker, *Phys. Lett. B* 419 (1998) 419.
14. T. Sjstrand, *hep-ph/9508391*.
15. G. M. Arnesini et al., *hep-ph/9607393*.
16. I. G. Knowles and G. D. Laerly, *J. Phys. G* 23 (1997) 731, *hep-ph/9705217*.
17. R. K. Ellis, W. J. Stirling and B. R. Webber, *QCD and Collider Physics*, Cambridge University Press (1996).
18. S. Bethke, J. E. Pilcher, *Ann. Rev. Nucl. Part. Sci.* 42 (1992) 251.
19. T. Hebbeker, *Phys. Rep.* 217 (1992) 217.
20. S. Bethke, *Proc. of the 42nd Scottish Universities Summer School in Physics, St. Andrews 1993*, in: *High Energy Phenomenology*, edited by K. Peach and L. V. Ick, SUSSP Publications and IOP Publishing (1994);
preprint HD-PY 93/7.

21. S.G. Gorishny, A.L. Kataev and S.A. Larin, Phys. Lett. B 259 (1991) 144;
L.R. Surguladze, M.A. Samuel, Phys. Rev. Lett. 66 (1991) 560.
22. T. Hebbeker, M. Martinez, G. Passarino and G. Quast, Phys. Lett. B 331 (1994) 165.
23. JADE Collab., W. Bartel et al., Z. Phys. C 33 (1986), 23;
JADE Collab., S. Bethke et al., Phys. Lett. B 213 (1988), 235.
24. Yu.L. Dokshitzer, Contribution to the Workshop on Jets at LEP and HERA, Durham (1990), J. Phys. G 17 (1991).
25. Z. Kunszt and P. Nason [conv.] in Z Physics at LEP 1 (eds. G. Altarelli, R. Kleiss and C. Verzegnassi), CERN 89-08 (1989).
26. S. Bethke, Z. Kunszt, D.E. Soper and W.J. Stirling, Nucl. Phys. B 370 (1992) 310.
27. Yu.L. Dokshitzer, G.D. Leder, S. Moretti and B.R. Webber, JHEP 9708:001, 1997; hep-ph/9707323.
28. S. Bentvelsen and I. Meyer, Eur. Phys. J C 4 (1998) 623.
29. S. Bethke, Proc. QCD Euroconference 96, Montpellier, France, July (1996), Nucl. Phys. (Proc. Suppl.) 54A (1997) 314; hep-ex/9609014.
30. S. Catani, L. Trentadue, G. Tumock and B.R. Webber, Nucl. Phys. B 407 (1993) 3.
31. L3 Collaboration, M. Acciarri et al., Phys. Lett. B 411 (1997) 339.
32. P.A. M. ovilla-Fernandez, O. Biebel and S. Bethke, hep-ex/9906033.
33. S. Bethke, IVth Int. Symp. on Radiative Corrections, Barcelona, Sept. 8-12, 1998; hep-ex/9812026.
34. K.G. Chetyrkin et al., hep-ph/9706430.
35. M. Schmelling, Phys. Scripta 51 (1995) 676.

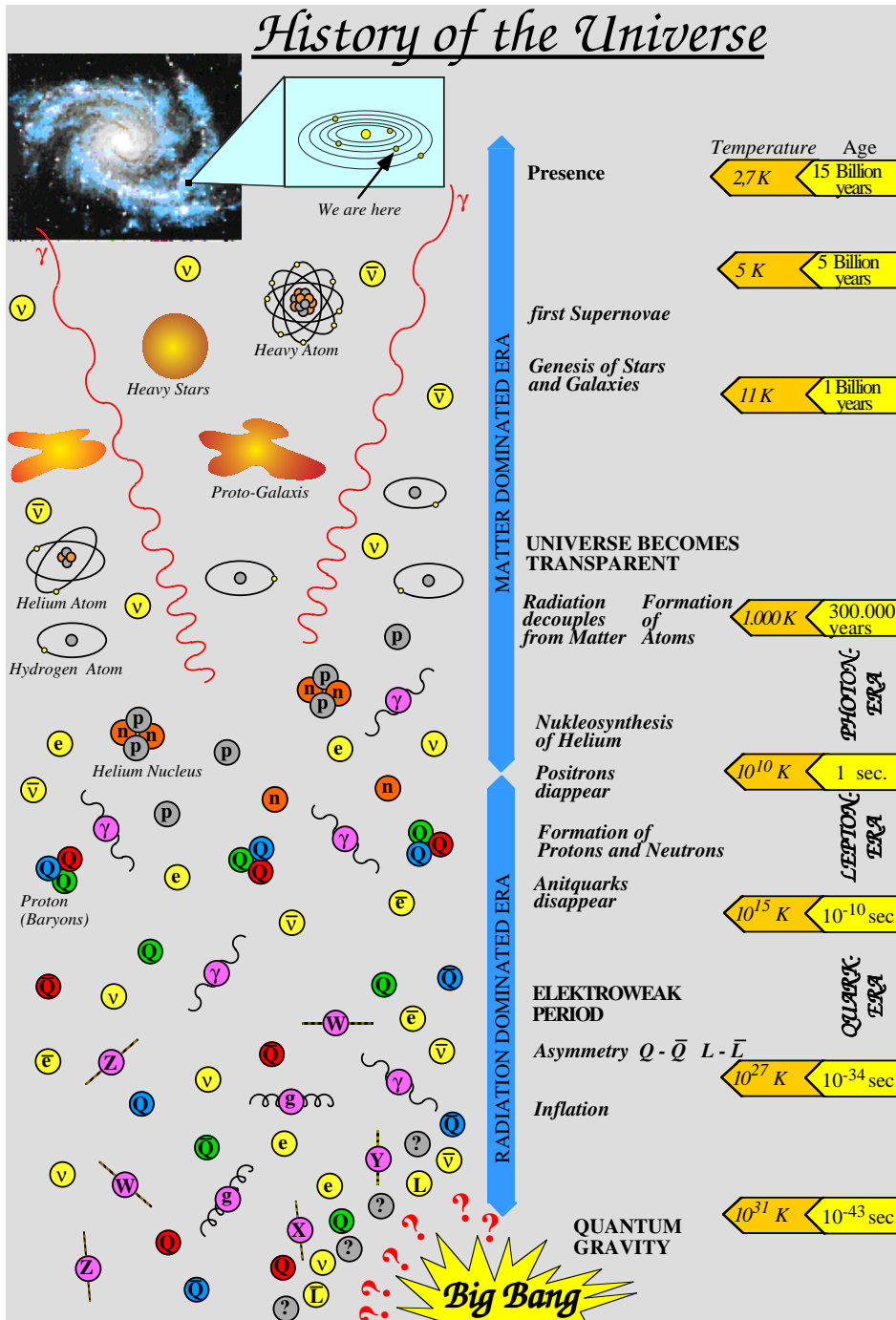


Figure 1.

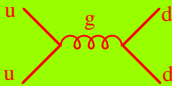
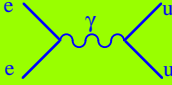
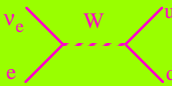
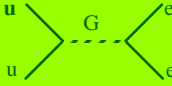
Fundamental Particles and Interactions:

Fundamental Fermions:

	Families			electric charge	Forces			
	u d	c s	t b		str	em	weak	grav
Quarks	u	c	t	2/3	x	x	x	x
	d	s	b	-1/3	x	x	x	x
Leptons	ν_e	ν_μ	ν_τ	0	-	-	x	?
	e	μ	τ	-1	-	x	x	x

} plus respective anti-particles

Fundamental Forces:

Interaction	exchanged boson	relative strength	example
Strong	Gluon (g)	1	
Electromagnet.	Photon (γ)	$\frac{1}{137}$	
Weak	W^+ , W^- , Z^0	10^{-14}	
Gravitation	Graviton (G) ?	10^{-40}	

Spontaneous Symmetry Breaking and generation of masses:

→ Higgs-particle (H) ; as yet, unobserved.

Figure 2.

Parameters of LEP

	LEP-I	LEP-II
max. beam energy	55 GeV	≈ 100 GeV
field of dipole magnets	0.065 T	0.111 T
acceleration voltage per turn	260 MeV	2700 MeV
Clystron Power	16 MW	16 MW
Cavities	Cu (warm) 128 in P2 und P6	Cu-Nb (supracond.) 288 in P2,4,6,8
acceleration voltage	1.5 MV/m	6 MV/m
beam currents	3 mA	5 mA
number of e ⁺ e ⁻ bunches	4 x 4	4 x 4 (x 2 bunchlets)
max. luminosity	1.6 · 10 ³¹ cm ⁻² s ⁻¹	5 · 10 ³¹ cm ⁻² s ⁻¹
energy spread	40 MeV	280 MeV
sys. error on beam energy	1.4 MeV	25-30 MeV
beam lifetime	≈ 6 - 8 h	≈ 5 h

Energy calibration:

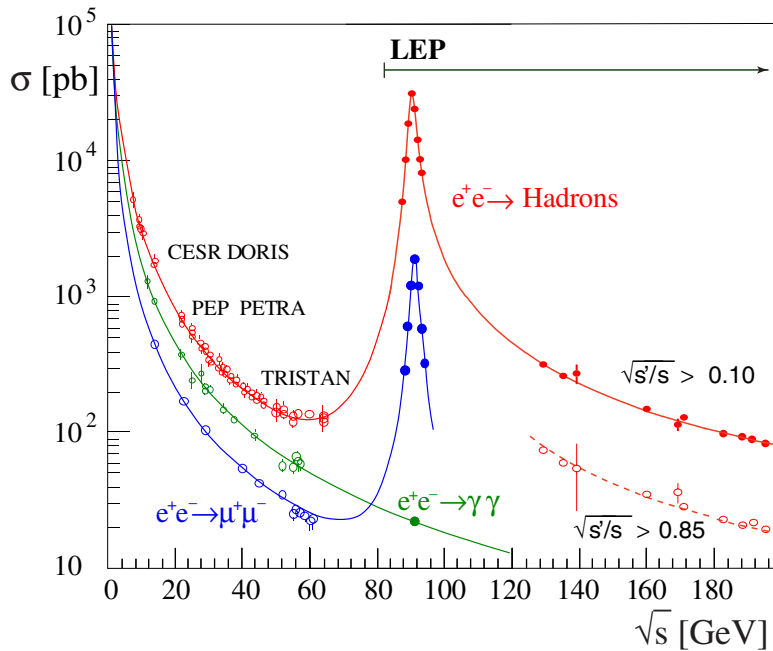
by **resonant depolarisation** of the beam polarisation (which builds up itself through emission of synchrotron radiation [bremsstrahlung]); executed at suitable beam energies (e.g. at about 55 GeV), plus extrapolation to higher energies using flux-loop measurements.

beam energy now: (fall 1999)

101 GeV → $\sqrt{s} = 202$ GeV

Figure 3.

cross sections of e^+e^- Annihilations at LEP



LEP-I:

- 17.000.000 Z^0 - decays recorded at $\sqrt{s} \approx M_Z = 91.2$ GeV
 \Rightarrow precision tests of the electroweak and strong interactions

LEP-II:

- data at $\sqrt{s} = 130 \dots > 200$ GeV (\sqrt{s} : hadronic c.m. energy)
 \Rightarrow tests of Standard Model and search for new physics
 \Rightarrow production of W^+W^- and of ZZ events

Figure 4.

e^+e^- Annihilation Final States at LEP

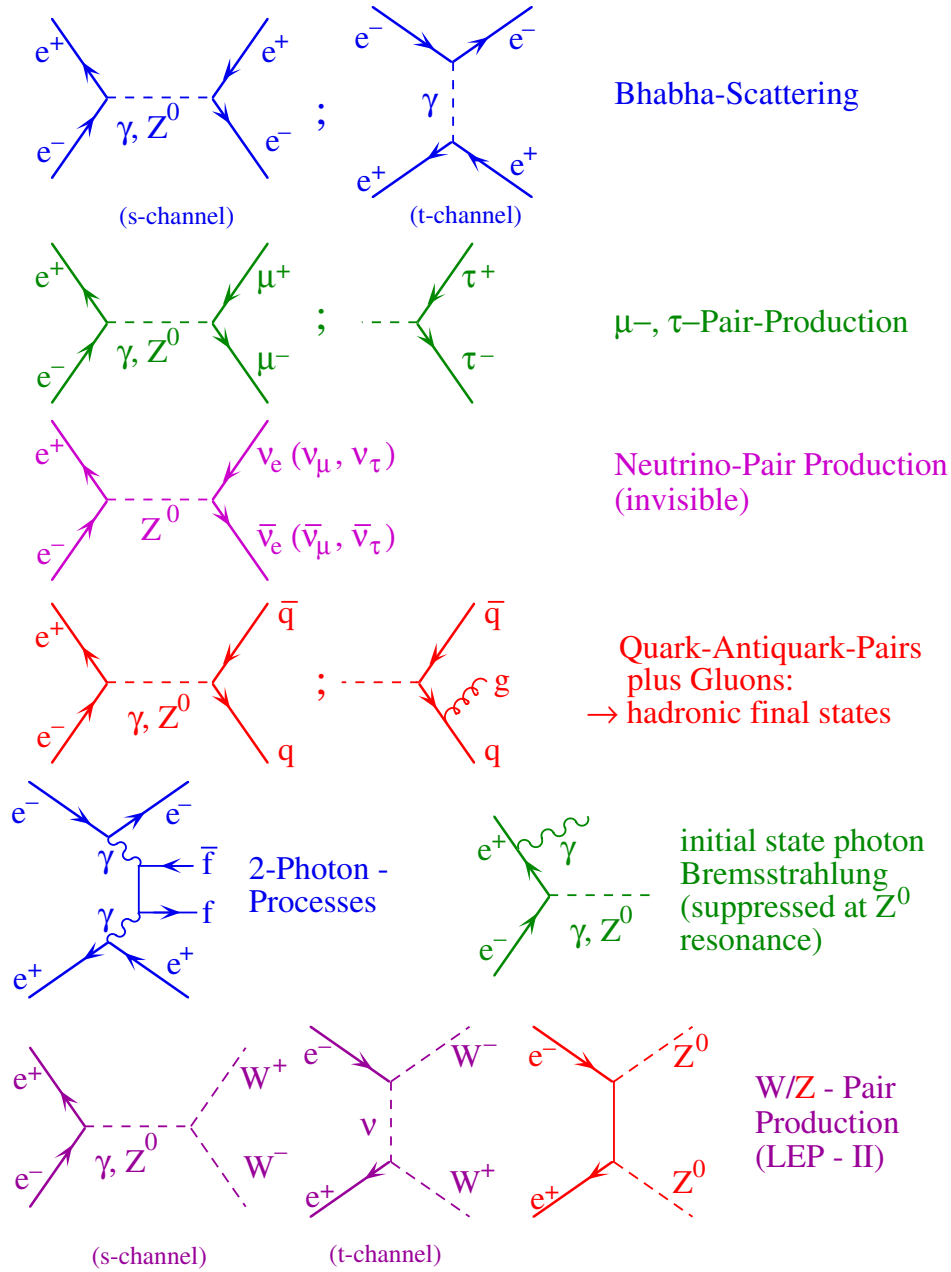


Figure 5.

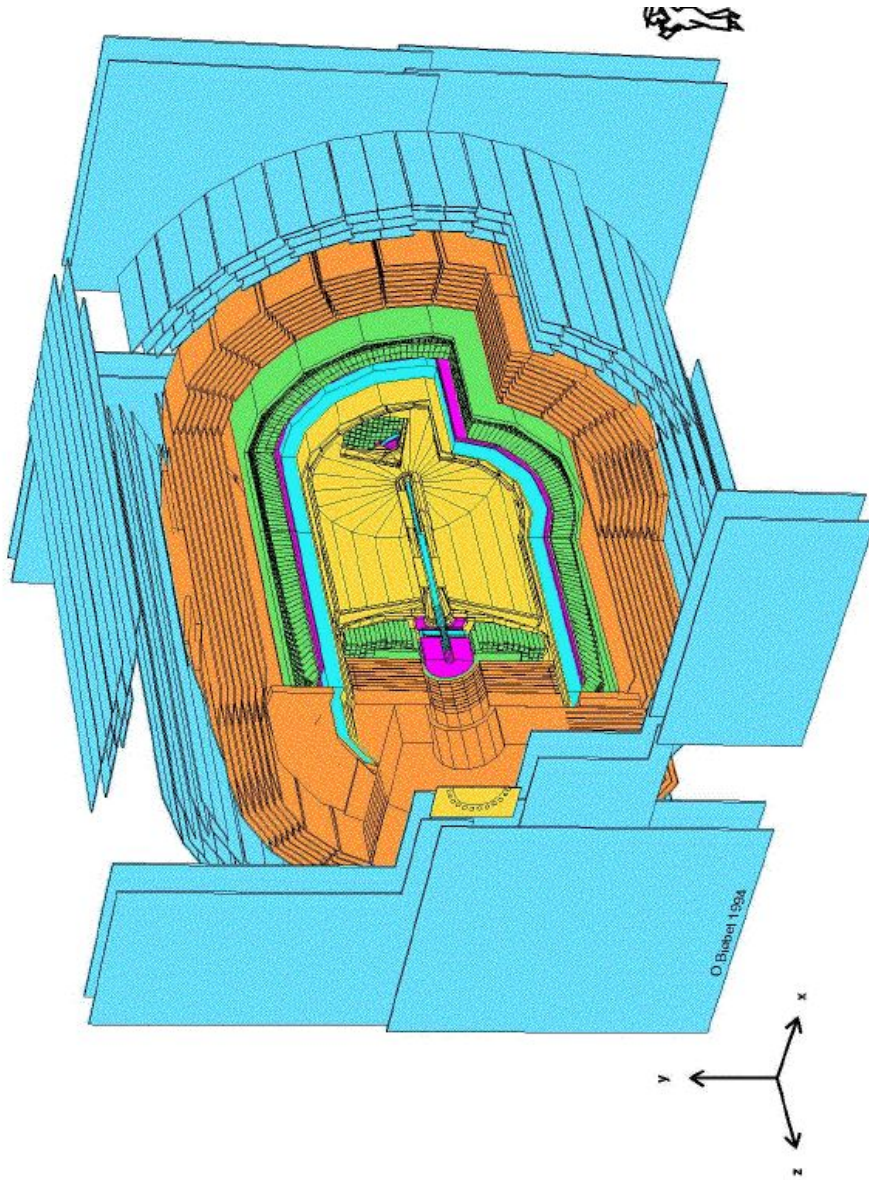


Figure 6.

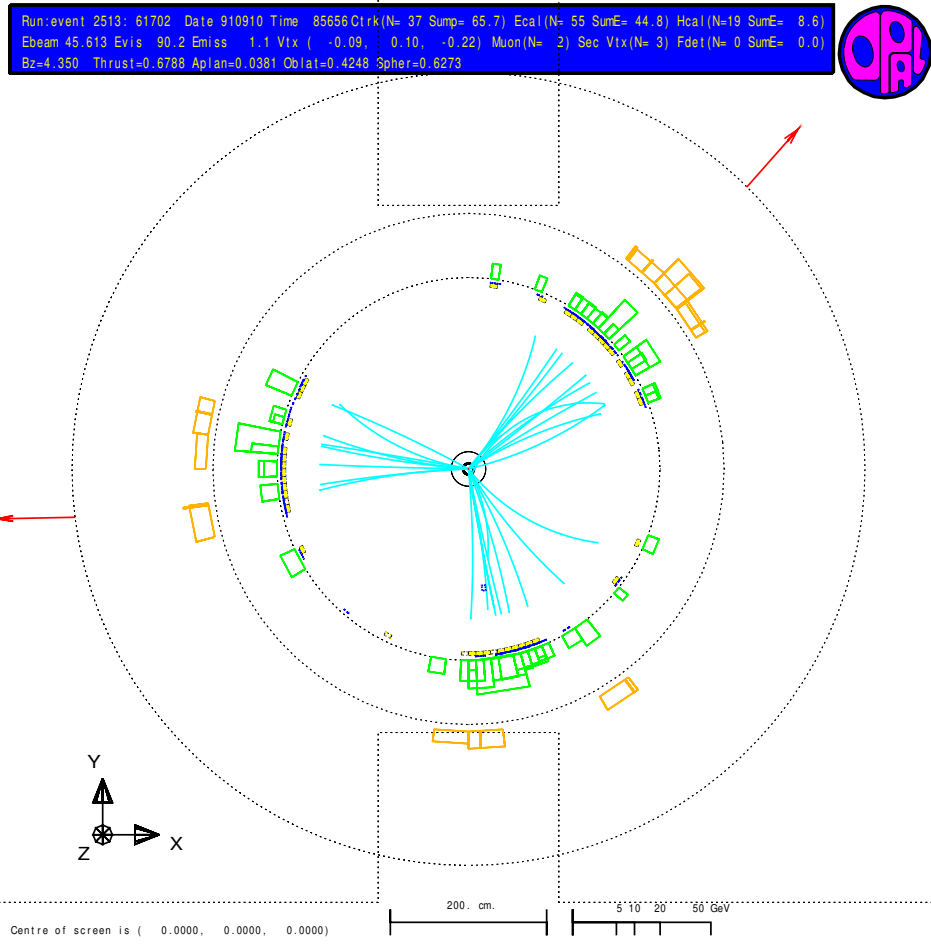


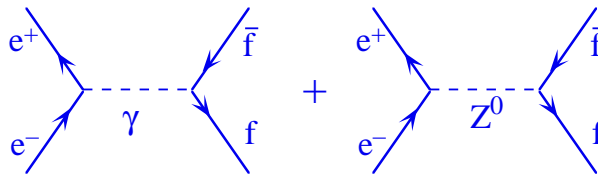
Figure 7.

Z^0 -Resonance and the Standard Model of Electroweak Interactions

minimal SM in lowest order („Born Approximation“) describes processes like $e^+e^- \rightarrow f\bar{f}$ using only 3 free parameters:

- α [fine structure constant]
- G_F [Fermi constant; from μ lifetime]
- $\sin^2\theta_w$ [weak mixing angle; from ν -N-scattering]

or: α , G_F and M_Z (since $\sin^2\theta_w \cos^2\theta_w = \frac{\pi\alpha}{G_F\sqrt{2}M_Z^2}$)



- $(f, \bar{f}) \equiv (e^+, e^-), (\mu^+, \mu^-), (\tau^+, \tau^-);$
 $(\nu_e, \bar{\nu}_e), (\nu_\mu, \bar{\nu}_\mu), (\nu_\tau, \bar{\nu}_\tau);$
 $(u, \bar{u}), (c, \bar{c}), (t, \bar{t});$
 $(d, \bar{d}), (s, \bar{s}), (b, \bar{b}).$

cross sections around Z^0 resonance ($f \neq e$):

$$\sigma_f(s) = \sigma_f^0 \cdot \frac{s\Gamma_Z}{(s-M_Z^2)^2 + M_Z^2\Gamma_Z^2} + \text{"}\gamma\text{"} + \text{"}\gamma Z\text{"}$$

$$\sigma_f^0 = \frac{12\pi}{M_Z^2} \cdot \frac{\Gamma_e \Gamma_f}{\Gamma_Z^2} \quad (\text{pole cross sections; } \sum \Gamma_f = \Gamma_Z)$$

Figure 8.

Measurement of s-dependent cross sections around the Z^0 resonance and adjustment of $\sigma_f(s)$, σ_f^0 provides **model independent** results for:

$$M_Z, \Gamma_Z, \Gamma_f, \sigma_f^0.$$

\mathcal{SM} : Γ_f are no free parameters, they are parametrised as functions of the *vector* and *axial vector constants*:

$$\Gamma_f = \frac{G_f M_Z^3}{6\pi \sqrt{2}} \cdot [g_{a,f}^2 + g_{v,f}^2] \cdot N_{c,f} \quad \left\{ \begin{array}{l} \text{colour factor; } \equiv 3 \text{ for quarks,} \\ \equiv 1 \text{ for leptons.} \end{array} \right.$$

$$g_{a,f} = I_{3,f} \quad (\text{3rd component of weak isospin; } = \pm 1/2)$$

$$g_{v,f} = I_{3,f} - 2 Q \sin^2\theta_w$$

Radiative Corrections:

- **photonic:**

→ corrections $\approx 100\%$; depending on event selection;
factorise: $\Rightarrow (1 + \delta_{rad})$

- **non-photonic:**

→ corrections $\approx 10\%$; independent of event selection;
 \Rightarrow can be absorbed in „*running coupling constants*“

Figure 9.

Running coupling constants:

- $\sin^2\theta_{\text{eff}}(s)$
- $\alpha(s) = \frac{\alpha}{1 - \Delta\alpha}$ ($\Delta\alpha \approx 1.064$ at $\sqrt{s} = M_Z$)
- $N_{c,f} \cdot \left(1 + \frac{\alpha_s}{\pi} + 1.4 \left(\frac{\alpha_s}{\pi} \right)^2 + \dots \right)$ (for quarks)
- $\frac{M_W^2}{M_Z^2} = \rho \cdot \cos^2 \theta_w$
- $\rho = \frac{1}{1 - \Delta\rho}$; $\Delta\rho = 0.0026 \cdot \frac{M_t^2}{M_Z^2} - 0.0015 \cdot \ln\left(\frac{M_H}{M_W}\right)$



insert running coupling constants into Born-approximation



partial widths will depend on:

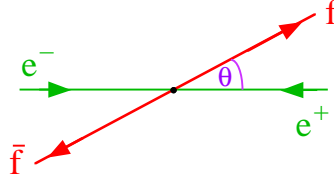
- M_t (top-quark mass)
- M_H (Higgs mass)
- α_s (strong coupling ,constant')

Figure 10.

Further Observables to be measured:

- **differential** cross sections:

$$\frac{d\sigma_f}{d\cos\theta} \propto A \cdot (1 + \cos^2\theta) + B \cdot \cos\theta$$



A and B include terms for γ - and Z^0 -exchange as well as for γ - Z^0 -interference, which depend on

$$\left(g_{a,e}^2 + g_{v,e}^2\right), \left(g_{a,f}^2 + g_{v,f}^2\right), \left(g_{a,e} \cdot g_{a,f}\right), \left(g_{v,e} \cdot g_{v,f}\right), \text{ and on}$$

the relativistic Breit-Wigner resonance, $\frac{s}{s - M_Z^2 + is\Gamma_Z / M_Z}$.

- forward-backward **asymmetries:**

$$A_{FB} = \frac{N_F - N_B}{N_F + N_B}$$

N_F : number of events with $\theta < \pi/2$
 N_B : number of events with $\pi/2 < \theta < \pi$

on the Z^0 pole: $A_{FB}^{0,f} = \frac{3}{4} \mathcal{A}_e \mathcal{A}_f$

$$\text{with } \mathcal{A}_f = \frac{2g_{v,f} \cdot g_{a,f}}{g_{v,f}^2 + g_{a,f}^2} \left[\approx \frac{g_{v,f}}{g_{a,f}} \text{ for leptons} \right]$$

- final state **polarisations** of leptons:

$$\mathcal{P}_f = \frac{1}{\sigma_{\text{tot}}} \cdot (\sigma_f(h=+1) - \sigma_f(h=-1))$$

$$\mathcal{P}_f(s = M_Z) = -\mathcal{A}_f$$

$$A_{FB}^{\mathcal{P}_f}(s = M_Z) = -\frac{3}{4} \mathcal{A}_e$$

Figure 11.

Precision Tests of the Standard Model from LEP:

(preliminary; summer 1999)

- experiments measure $\sigma_f(s)$, A_{FB}^f , \mathcal{P}_f , $A_{\text{FB}}^{\mathcal{P}_f}$
- data of 4 experiments are combined by
„LEP Electroweak Working Group“
- common fit to combined data

↓ (LEP-I)

$$M_Z = 91187.2 \pm 2.1 \text{ MeV} \quad \text{n.b.: 23 ppm !!}$$

$$\Gamma_Z = 2499.4 \pm 2.4 \text{ MeV}$$

$$\sigma_{\text{had}}^0 = 41.544 \pm 0.037 \text{ nb}$$

$$\Gamma_{\text{had}} = 1743.9 \pm 2.0 \text{ MeV}$$

$$\Gamma_{\text{lept}} = 83.96 \pm 0.09 \text{ MeV}$$

$$\Gamma_{\text{invis}} = 489.8 \pm 1.5 \text{ MeV}$$

$$\Rightarrow N_\nu = 2.9835 \pm 0.0083$$

from radiative corrections :

LEP I & II

LEP & SLD & pp & νN

$$M_{\text{top}} = 172_{-11}^{+14} \text{ GeV}$$

$$173.6 \pm 4.3 \text{ GeV}$$

$$M_{\text{H}} = 143_{-87}^{+284} \text{ GeV}$$

$$92_{-45}^{+78} \text{ GeV}$$

$$\alpha_s(M_Z) = 0.120 \pm 0.003 \pm 0.002$$

$$0.119 \pm 0.003 \pm 0.002$$

$$\sin^2 \theta_{\text{lept}}^{\text{eff}} = 0.23187 \pm 0.00021$$

$$0.23159 \pm 0.00016$$

$$M_{\text{W}} = 80.340 \pm 0.032 \text{ GeV}$$

$$80.377 \pm 0.022 \text{ GeV}$$

Figure 12.

Tampere 1999

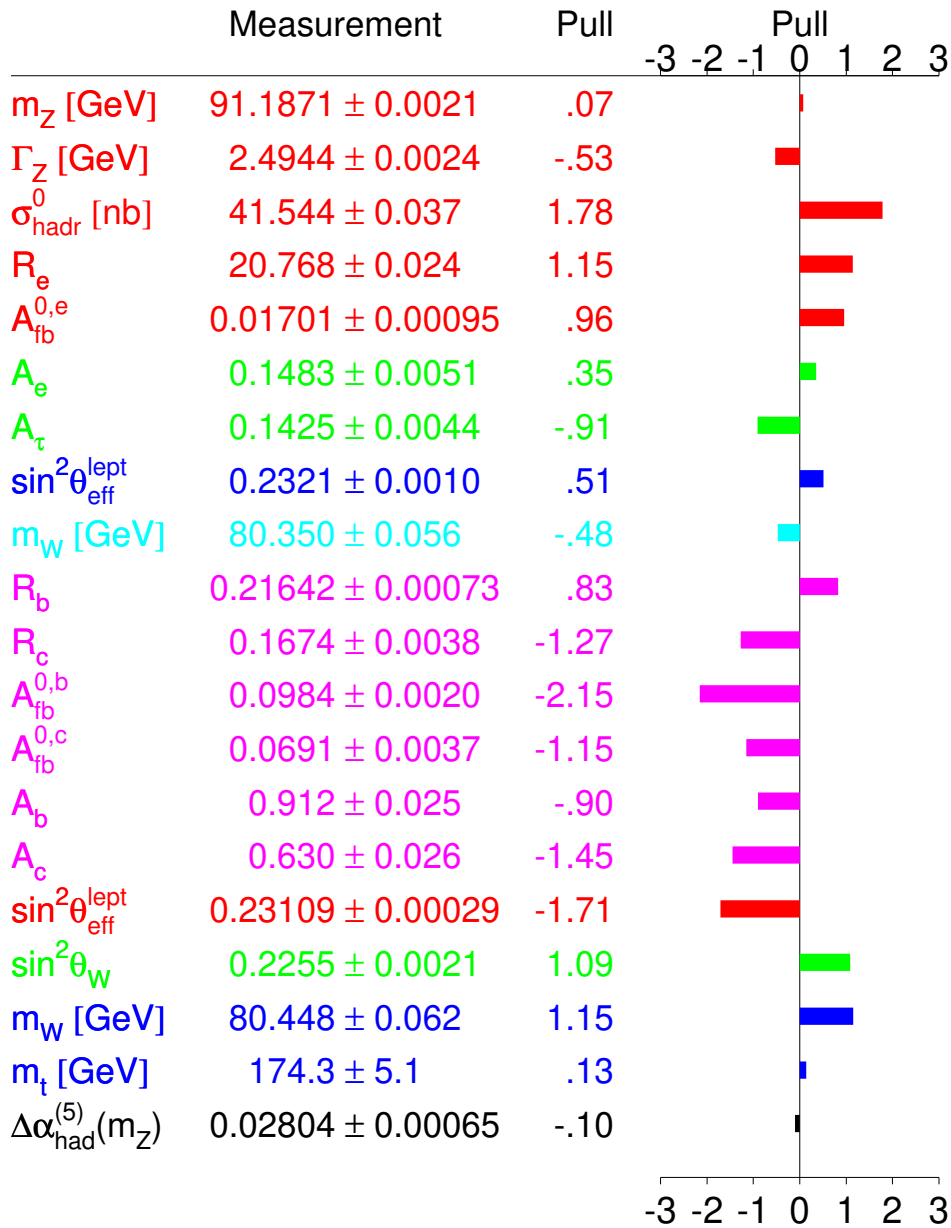


Figure 13.

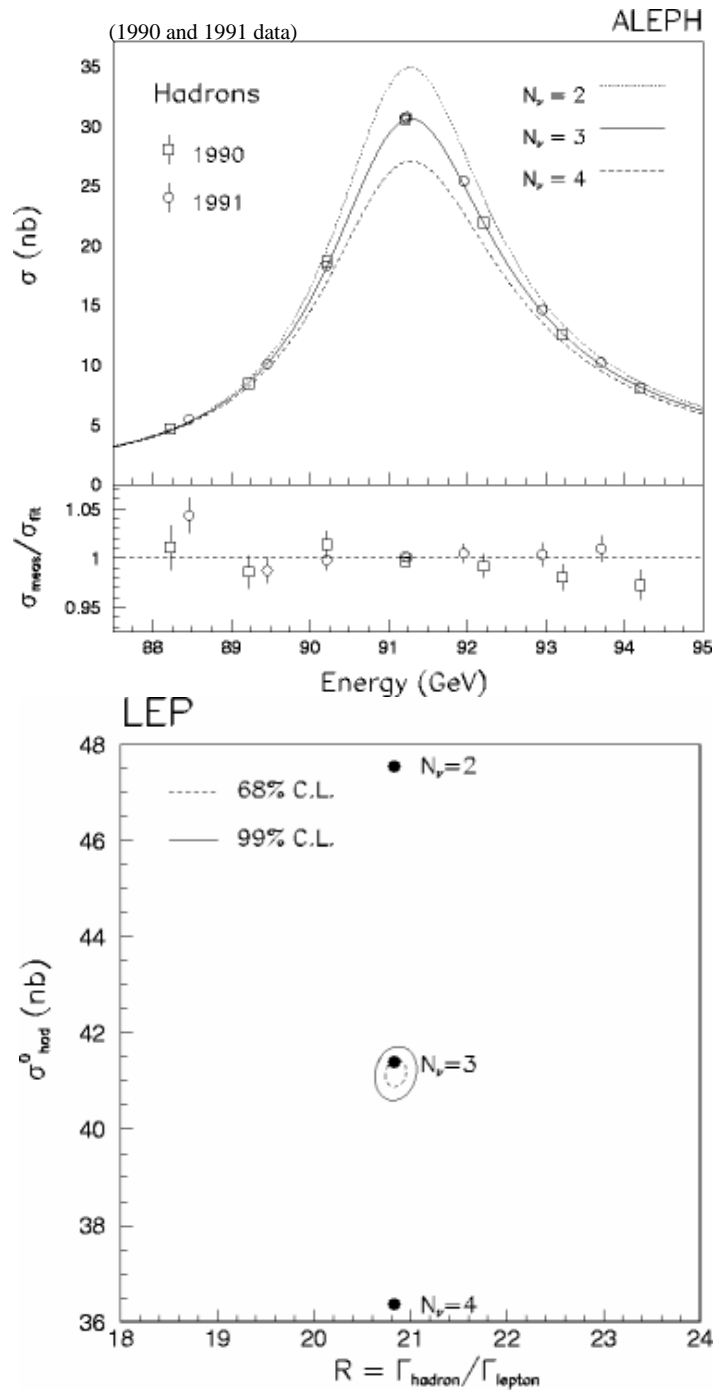


Figure 14.

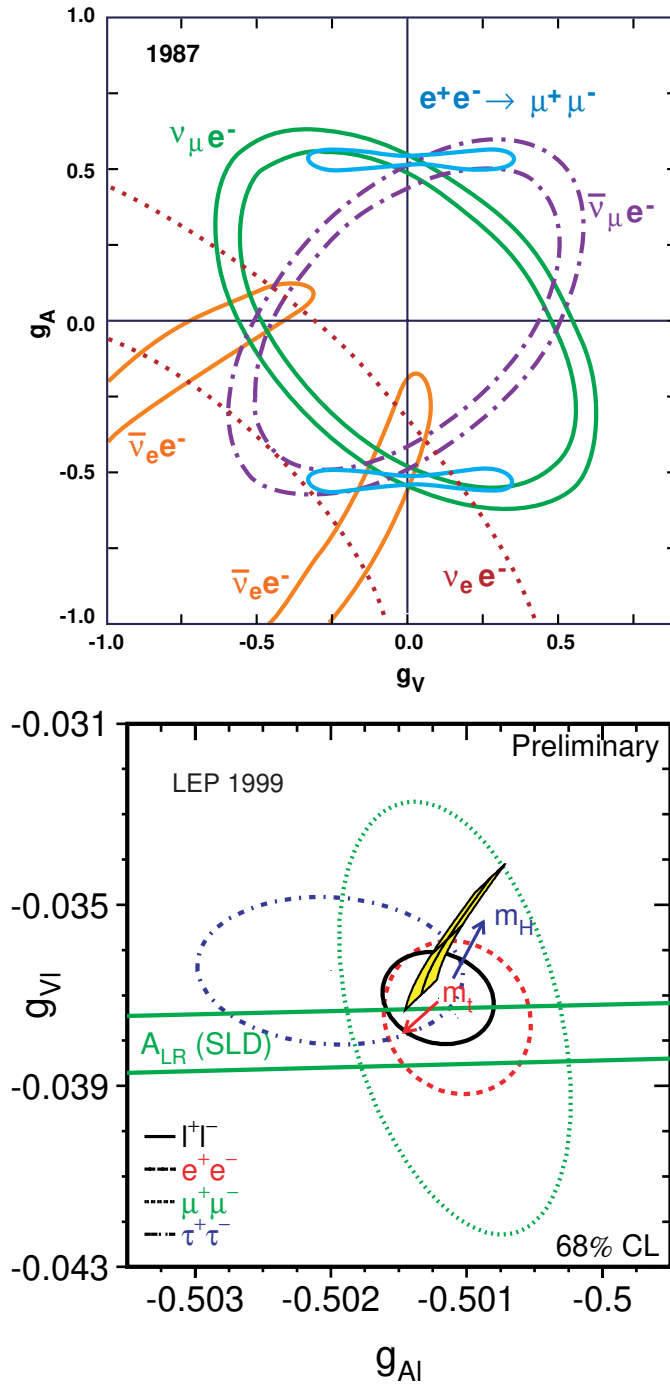


Figure 15.

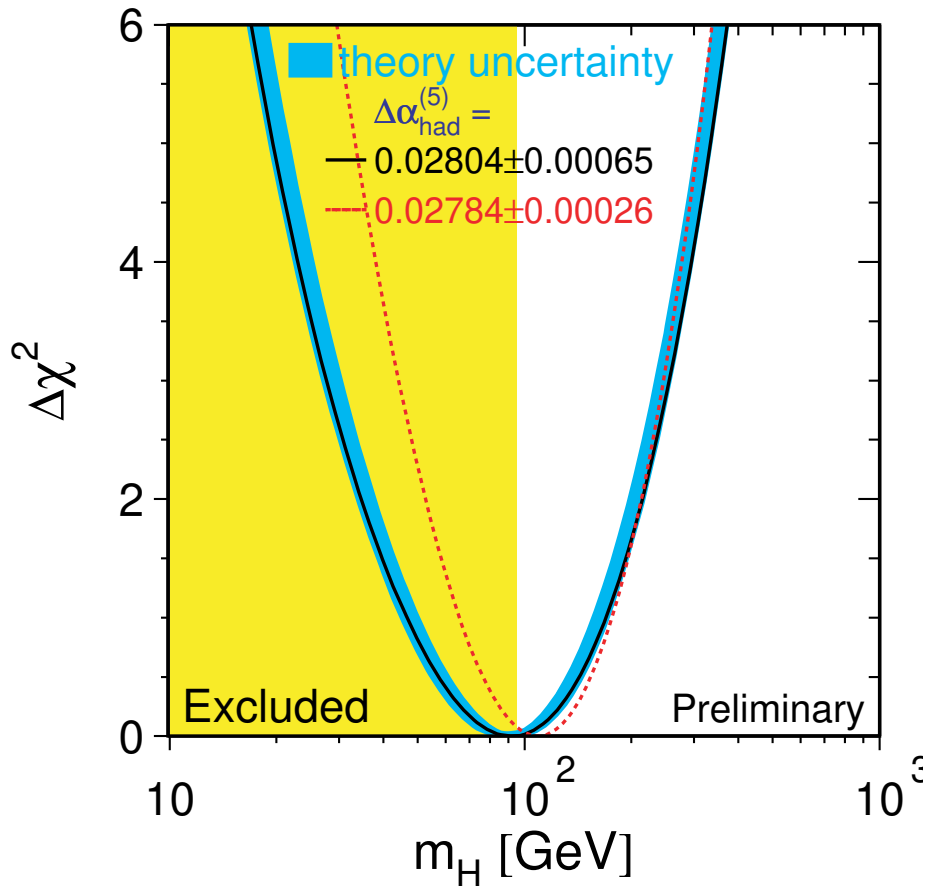


Figure 16.

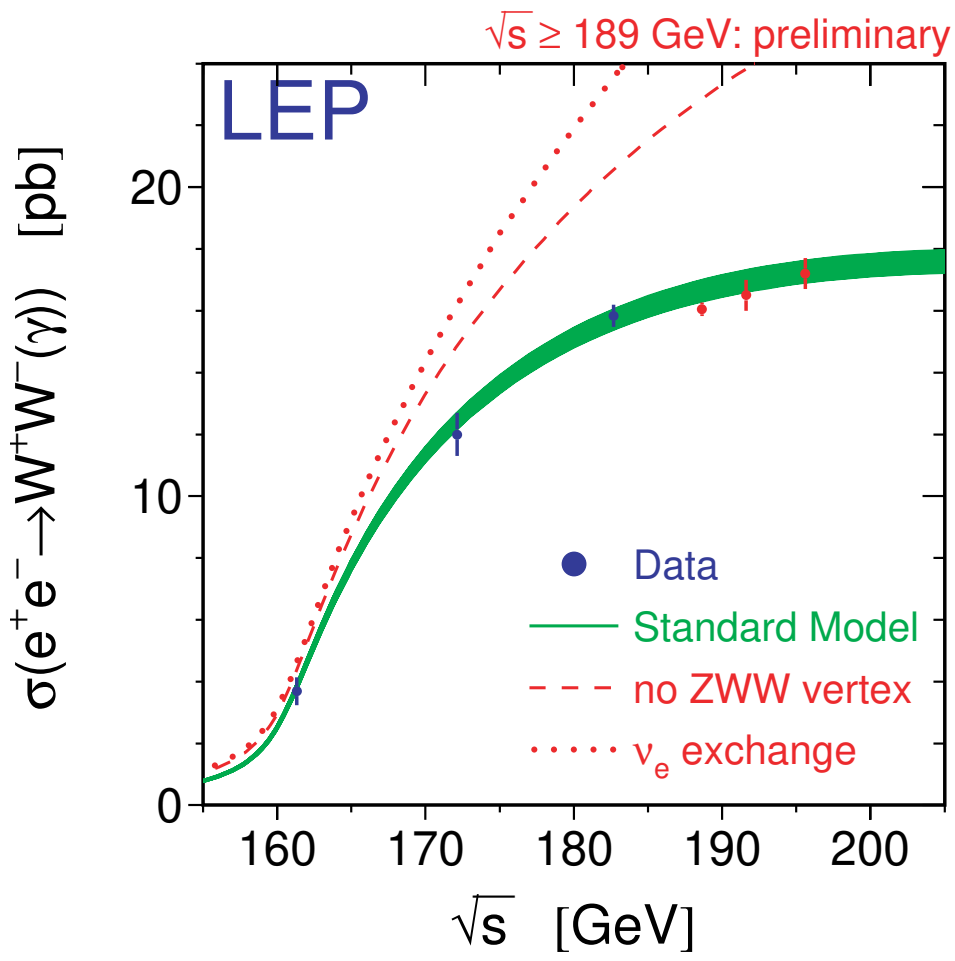


Figure 17.

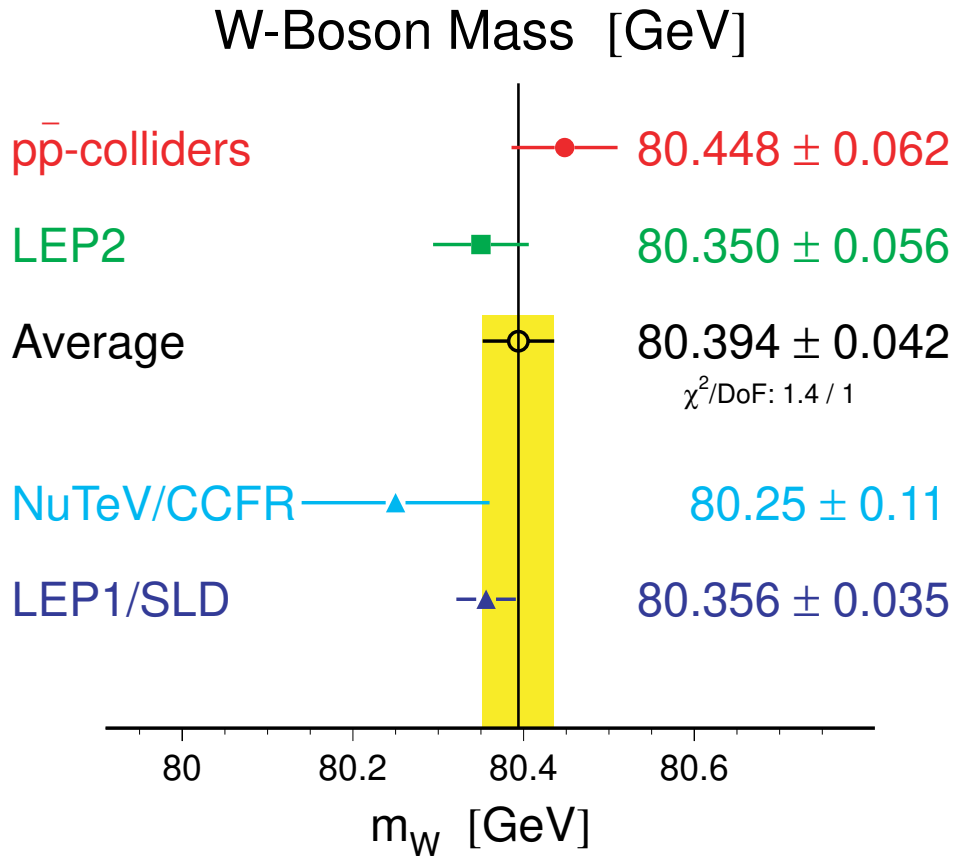
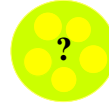


Figure 18.

Short History of Hadron Physics

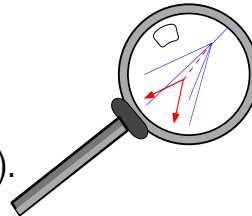
1932: Discovery of the **neutron**

1933: $\vec{\mu}_p \cong 2.5 \frac{e}{2 m_p} \vec{\sigma} \Rightarrow$ **Substructure** of the proton

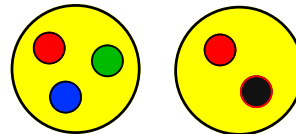


1947: Discovery of π -mesons and of long-lived V-particles (K^0, Λ) in **cosmic rays**

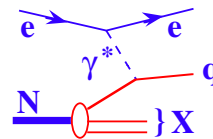
1953: V-particles produced at **accelerators**; new inner quantum number ("**strangeness**").



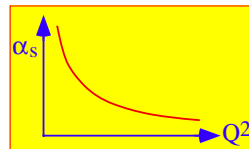
1964: Static **Quark-Model**; new inner quantum number: **color**.



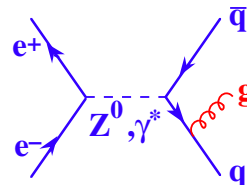
1969: Dynamic **Parton Model**:



1973: Concept of **Asymptotic Freedom**; non-abelian gauge theory: **QCD**.



1975: **2-Jet structure** in e^+e^- -annihilation: confirmation of **Quark-Parton-Model**.



1979: Discovery of the **gluon** in **3-Jet**-events of e^+e^- -annihilation.

Figure 19.

Properties of QED and of QCD:


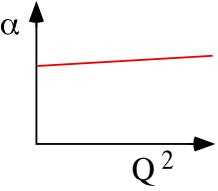
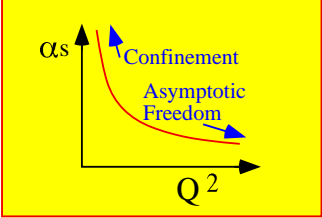
	QED	QCD
<i>fermions</i>	<i>leptons (e, μ, τ)</i>	<i>quarks (u, d, s, c, b, t)</i>
<i>force couples to</i>	<i>electric charge</i>	3 color charges
<i>exchange quantum</i>	<i>photon (γ) (carries no charge)</i>	<i>gluons (g) (carry 2 color charges)</i> ⇒  is possible
<i>coupling constant:</i>	$\alpha(Q^2 = 0) = \frac{1}{137}$ 	$\alpha_s(Q^2 = M_Z^2) \approx 0.12$ 
<i>free particles</i>	<i>leptons (e, μ, τ)</i>	hadrons (colorless bound states of q and q̄)
<i>theory</i>	<i>perturbation theory up to O(α⁴)</i>	<i>pert. theory to O(α_s²) (some to O(α_s³)); leading log approx.</i>
<i>precision</i>	<i>10⁻⁶ 10⁻⁷</i>	<i>5% ... 20% (?)</i>

Figure 20.

Basics of QCD and of Hadron Production:

renormalisation scale dependence of α_s is controlled by " β -function":

$$\mu \frac{\partial \alpha_s}{\partial \mu} = -\frac{\beta_0}{2\pi} \alpha_s^2 - \frac{\beta_1}{4\pi^2} \alpha_s^3 - \dots \quad (1)$$

$$\beta_0 = \frac{11N_c - 2N_f}{3}$$

$$\beta_1 = \frac{17N_c^2 - 5N_c N_f - 3C_f N_f}{3}$$

QCD group structure functions:

$$C_f = 4/3$$

$$N_c = 3 \text{ (# of colours)}$$

$$N_f = \text{\# of quark flavours}$$

Solving (1) \Rightarrow introduction of a **constant** of integration.

\downarrow
not given by QCD

\rightarrow Experiment!

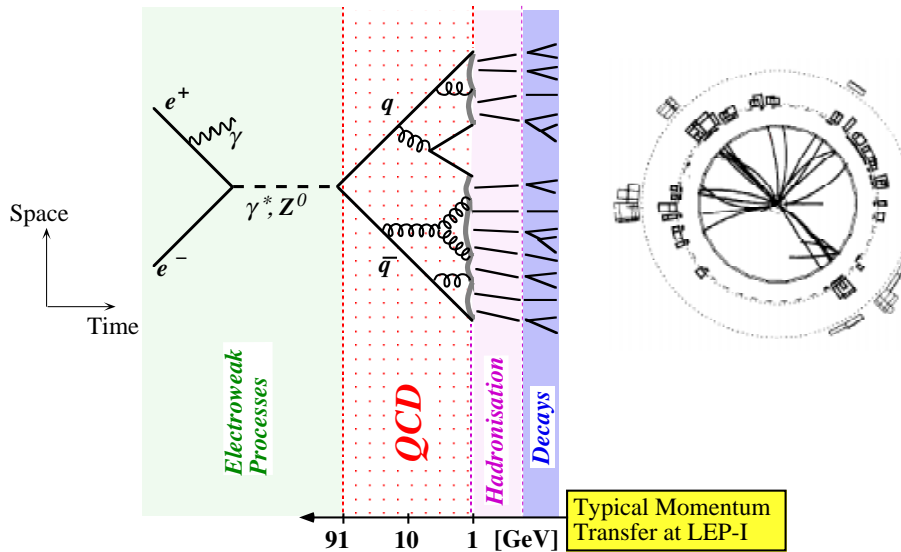
$$\alpha_s(\mu) = \frac{12\pi}{(33 - 2N_f) \ln\left(\frac{\mu}{\Lambda_{\overline{MS}}}\right)^2} \left[1 - 6 \frac{153 - 19N_f}{(33 - 2N_f)^2} \frac{\ln\left(\ln\left(\frac{\mu}{\Lambda_{\overline{MS}}}\right)^2\right)}{\ln\left(\frac{\mu}{\Lambda_{\overline{MS}}}\right)^2} + O(\alpha_s^3) \right]$$

Asymptotic Freedom: $\alpha_s \rightarrow 0$ if $\mu \rightarrow \infty$

Figure 21.

Anatomy of the Process $e^+e^- \rightarrow Z^0 \rightarrow \text{Hadrons}$

(QCD- and Hadronisation Models)



- **QCD:** *shower development calculated in Perturbation Theory [(next-to-) leading log approximations or fixed order]*
 - **Hadronisation:** *string- or cluster - fragmentation models*
-
- models used to study detector acceptance and hadronisation effects
 - analytic calculations used to extract physics results [α_s, \dots]
 - more recently: hadronisation effects approximated by non-perturbative power-suppressed ($1/Q$) contributions

Figure 22.

QCD Topics at LEP

◆ *Determinations of α_s*

- α_s from jet rates and hadronic event shapes
- α_s from hadronic decay width of the Z_0
- α_s from τ lepton decays
- α_s from scaling violations of fragmentation functions

◆ *Studies of 3-jet Events*

- evidence for asymptotic freedom
- tests of the QCD 3-jet matrix element
- observation of quark-gluon differences
- string hadronisation effect
- QCD colour factors

◆ *Studies of 4-jet Events*

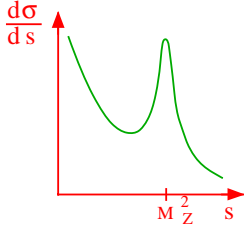
- colour factors and non-abelian gauge structure of QCD

◆ *Studies of Soft Gluon Coherence Effects*

◆ *General Properties of Hadronic Final States*

- event shape distributions ⇒
 - fragmentation functions
 - multiplicities
 - intermittency, factorial moments
 - Bose-Einstein correlations
- | | |
|---|---|
| } | hadronisation models
and power corrections |
| } | of various types
of particles |

$\alpha_s(M_Z)$ from Hadronic Z^0 Width



$$R_Z = \left(\frac{\Gamma_{\text{had}}}{\Gamma_{\text{lept}}} \right)_{\text{exp}} \equiv R_0 (1 + \delta_{\text{QCD}})$$

$$R_0 = 19.938^{+0.014}_{-0.013} \quad \left\{ \begin{array}{l} M_{\text{Higgs}} = 300^{+700}_{-220} \text{ GeV} \\ M_{\text{top}} = 174 \pm 5 \text{ GeV} \end{array} \right.$$

$$\delta_{\text{QCD}} = \left(\frac{\alpha_s}{\pi} \right) + 1.409 \left(\frac{\alpha_s}{\pi} \right)^2 - 12.767 \left(\frac{\alpha_s}{\pi} \right)^3$$

- + R_Z not affected by hadronisation effects (involves only 'simple' event counting).
- $\delta_{\text{QCD}} \sim 0.04 \Rightarrow$ high experimental precision needed.
- must assume validity of e.w. standard model

LEP average: $R_Z = 20.768 \pm 0.026$ (summer 1999)

$$\Rightarrow \alpha_s(M_Z) = 0.123 \pm 0.004 + 0.002 \pm 0.002$$

(exp.) (M_H, M_t) (QCD)

$$\Rightarrow \alpha_s(M_Z) = 0.123 \pm 0.005$$

From combined fit of line shapes and asymmetries:

$$\alpha_s(M_Z) = 0.120 \pm 0.003 \pm 0.002$$

$$M_{\text{top}} = 172^{+14}_{-11} \text{ GeV}$$

Figure 24.

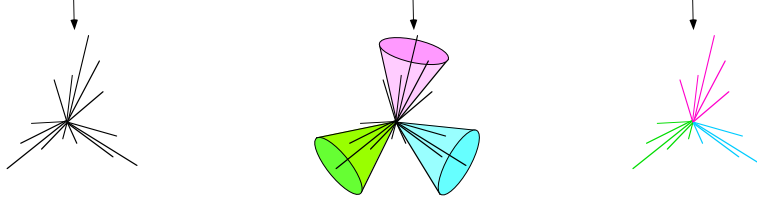
Physics of Hadron Jets

In order to compare Hadron Jets with analytic QCD-calculations (Quark- und Gluon Dynamics) one must define **resolvable particle jets**, both in theory and in experiment.

- Doing so one needs:
- definition of **resolution criteria** (e.g. minimal invariant pair masses, minimal angle, minimal energy ..)
 - procedure to **recombine** unresolvable jets.

There is no "natural" definition of Jets !

example: hadronic event with Cone-Algorithm or Inv. Mass Algor.



JADE jet definition: (most widely used in e^+e^- -annihilation)

2 groups of particles, i und j , can be resolved as individual jets if the scaled pair mass of the two, $y_{ij} = M_{ij}^2 / E_{cm}^2$, satisfies:

$$y_{ij} \geq y_{cut}$$

If $y_{ij} < y_{cut}$, the 'proto-jets' i and j will be replaced by a new, single (proto-) Jet k (recombination): $p_k = p_i + p_j$ (recursive procedure, until all $y_{ij} \geq y_{cut}$).

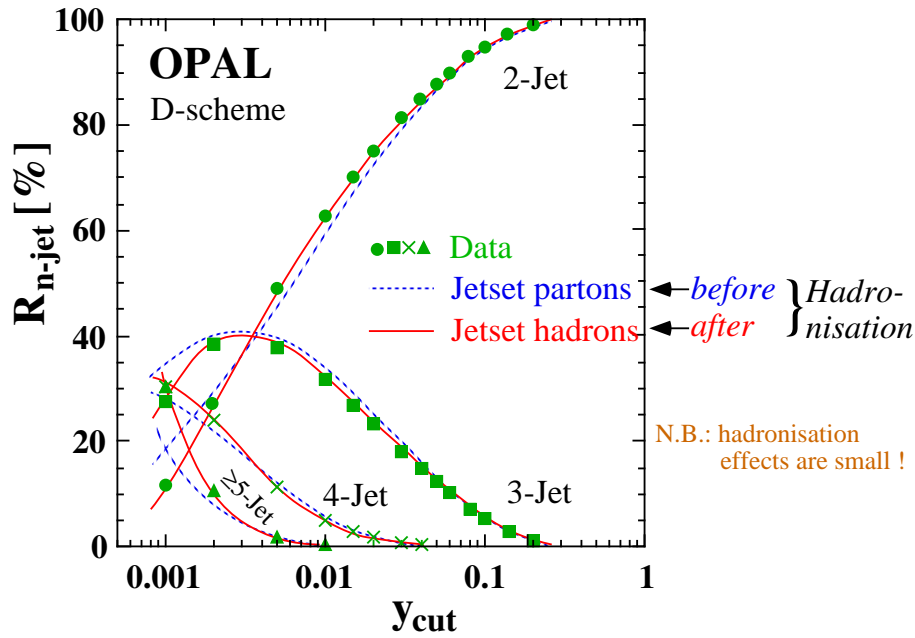
Figure 25.

JADE-type Jet Cluster Algorithms

Algorithm	Resolution y_{ij}	Recombination	Remarks
JADE	$\frac{2E_i E_j (1 - \cos \theta_{ij})}{s} [Y_{ij}^J]$	$p_k = p_i + p_j$	conserves E, p ; does not exponentiate
E	$\frac{(p_i + p_j)^2}{s}$	$p_k = p_i + p_j$	Lorentz invariant
E0	$\frac{(p_i + p_j)^2}{s}$	$E_k = E_i + E_j$; $p_k = \frac{E_k}{p_i + p_j} (p_i + p_j)$	conserves E , but violates p
p	$\frac{(p_i + p_j)^2}{s}$	$p_k = p_i + p_j$; $E_k = p_k j$	conserves p , but violates E
p0	$\frac{(p_i + p_j)^2}{s}$	$p_k = p_i + p_j$; $E_k = p_k j$	as p-scheme; E updated after each recomb.
Durham	$\frac{2 \ln(E_i^2/E_j^2) (1 - \cos \theta_{ij})}{s} [Y_{ij}^D]$	$p_k = p_i + p_j$	conserves E, p ; avoids exp. problems
Cambridge	$2(1 - \cos \theta_{ij})$; soft freezing if $Y_{ij}^D > Y_{cut}^D$	$p_k = p_i + p_j$	conserves E, p ; avoids exp. problems
Geneva	$\frac{8E_i E_j (1 - \cos \theta_{ij})}{9(E_i + E_j)^2}$	$p_k = p_i + p_j$	conserves E, p ; avoids exp. problems
LUCLUS	$\frac{2p_i p_j \sin^2(\theta_{ij}/2)}{p_i + p_j}$	$p_k = p_i + p_j$	conserves E, p ; uncalculable in pert. th.

TABLE 1.

- jet production rates (naturally) depend on the choice of a jet resolution parameter !
- larger y_{cut} values \Rightarrow fewer multijet events



jet rates provide the possibility to determine α_s ...

$$R_{n-jet} = \frac{\text{\# of } n\text{-jet events}}{\text{\# all hadronic events}}$$

$$= C_1(y_{cut}) \cdot \alpha_s(\mu) + C_2(y_{cut}) \cdot \alpha_s^2(\mu) + \dots$$

\swarrow \searrow
given by QCD calculations

... and to prove the energy dependence of α_s !

Figure 26.

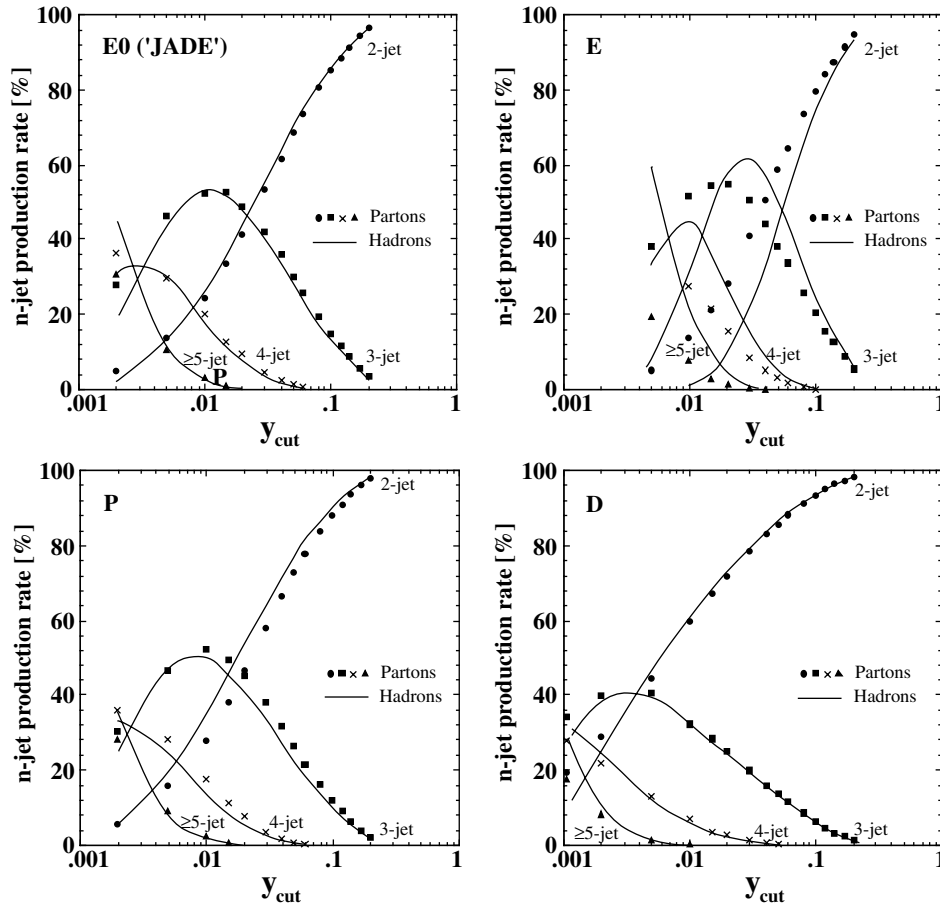


Figure 27.

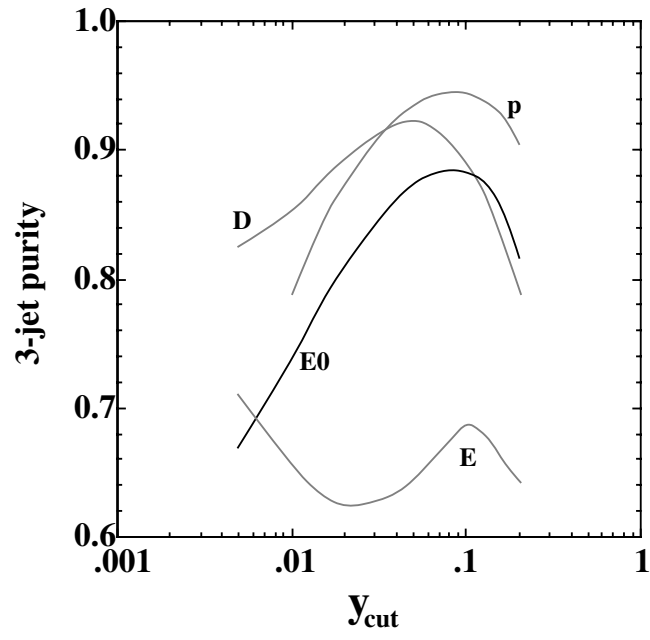


Figure 28.

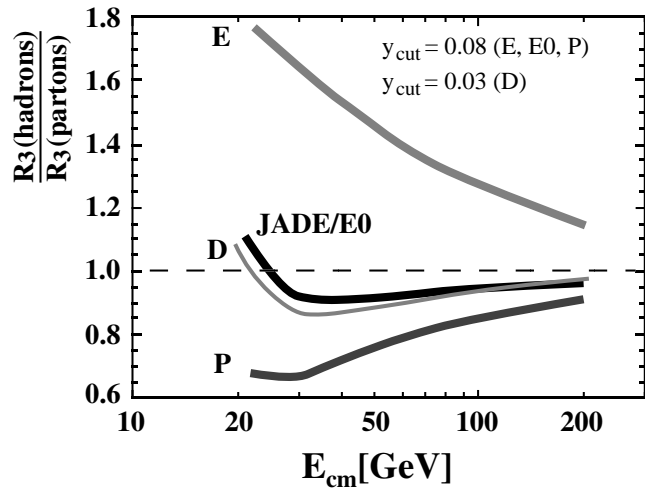


Figure 29.

Jet rates in e^+e^- annihilation:
direct test of asymptotic freedom

E0 (JADE) jet algorithm for $y_{\text{cut}} = 0.08$:
 (hadronisation corrections are small and energy
 independent for $E_{\text{cm}} > 30$ GeV)

$$R_3 \equiv \frac{\sigma_{3\text{-jet}}}{\sigma_{\text{tot}}} \propto \alpha_s(E_{\text{cm}}) \propto \frac{1}{\ln E_{\text{cm}}}$$

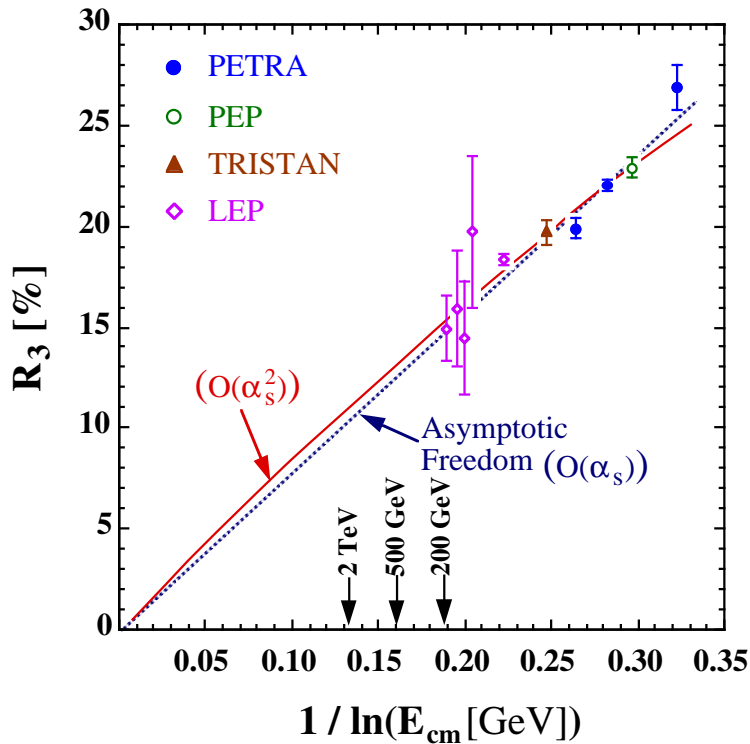


Figure 30.










Name of Observable	Definition	Typical Value for:			QCD calculation
					
Thrust	$T = \max_{\vec{n}} \left(\frac{\sum_i \vec{p}_i \cdot \vec{n} }{\sum_i \vec{p}_i } \right)$	1	$\geq 2/3$	$\geq 1/2$	(resummed) $O(\alpha_s^2)$
Thrust major	Like T, however T_{maj} and \vec{n}_{maj} in plane $\perp \vec{n}_T$	0	$\leq 1/3$	$\leq 1/\sqrt{2}$	$O(\alpha_s^2)$
Thrust minor	Like T, however T_{min} and \vec{n}_{min} in direction \perp to \vec{n}_T and \vec{n}_{maj}	0	0	$\leq 1/2$	$O(\alpha_s^2)$
Oblateness	$O = T_{\text{maj}} - T_{\text{min}}$	0	$\leq 1/3$	0	$O(\alpha_s^2)$
Sphericity	$S = 1.5 (Q_1 + Q_2)$; $Q_1 \leq \dots \leq Q_3$ are Eigenvalues of $S^{\alpha\beta} = \frac{\sum_i p_i^\alpha p_i^\beta}{\sum_i p_i^2}$	0	$\leq 3/4$	≤ 1	none (not infrared safe)
Aplanarity	$A = 1.5 Q_1$	0	0	$\leq 1/2$	none (not infrared safe)
Jet (Hemisphere) masses	$M_{\pm}^2 = \left(\sum_{i \in S_{\pm}} E_i^2 - \sum_i \vec{p}_i^2 \right)_{i \in S_{\pm}}$ (S_{\pm} : Hemispheres \perp to \vec{n}_T) $M_H^2 = \max(M_+^2, M_-^2)$ $M_D^2 = M_+^2 - M_-^2 $	0	$\leq 1/3$	$\leq 1/2$	(resummed) $O(\alpha_s^2)$
Jet broadening	$B_{\pm} = \frac{\sum_{i \in S_{\pm}} \vec{p}_i \times \vec{n}_T }{2 \sum_i \vec{p}_i }$; $B_T = B_+ + B_-$ $B_w = \max(B_+, B_-)$	0	$\leq 1/(2\sqrt{3})$	$\leq 1/(2\sqrt{2})$	(resummed) $O(\alpha_s^2)$
Energy-Energy Correlations	$EEC(\chi) = \sum_{\text{events}} \sum_{i,j} \frac{E_i E_j}{E_{\text{vis}}^2} \int_{\chi - \frac{\Delta\chi}{2}}^{\chi + \frac{\Delta\chi}{2}} \delta(\chi - \chi_{ij})$				(resummed) $O(\alpha_s^2)$
Asymmetry of EEC	$AEEC(\chi) = EEC(\pi - \chi) - EEC(\chi)$				$O(\alpha_s^2)$
Differential 2-jet rate	$D_2(y) = \frac{R_2(y - \Delta y) - R_2(y)}{\Delta y}$				(resummed) $O(\alpha_s^2)$

Figure 31.

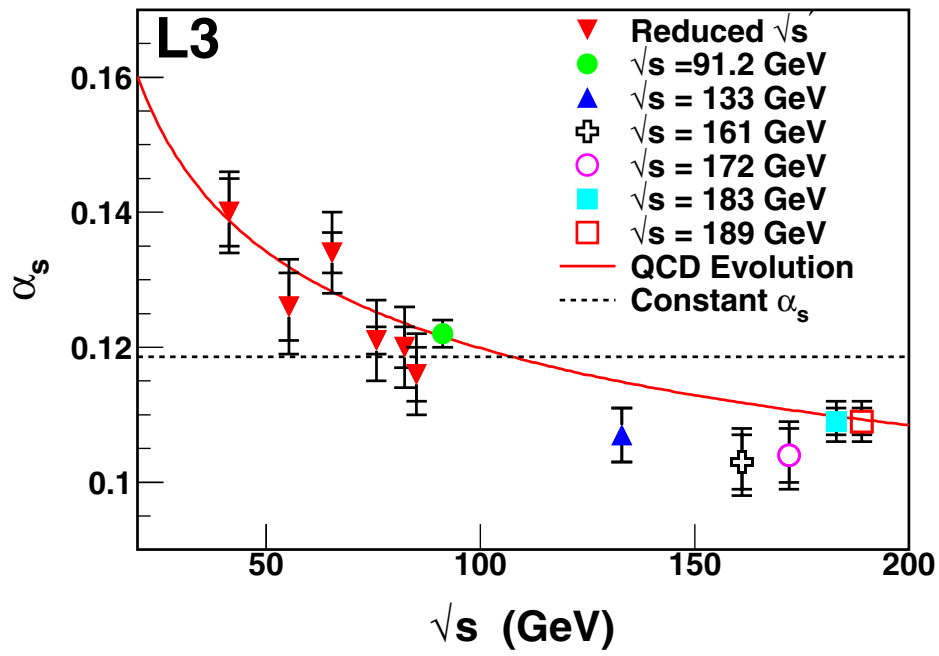


Figure 32.

Exp. Determination of α_s :

- in e^+e^- Annihilations:

- hadronic decays of Z Bosons⁰

$$R_Z = \frac{\Gamma(Z^0 \rightarrow \text{hadrons})}{\Gamma(Z^0 \rightarrow \mu^+\mu^-)} = R_0 \left(1 + \frac{\alpha_s}{\pi} + 1.4 \left(\frac{\alpha_s}{\pi} \right)^2 + \dots \right)$$

- hadronic decays of τ leptons

$$R_\tau = \frac{\Gamma(\tau \rightarrow \text{hadrons})}{\Gamma(\tau \rightarrow \mu\nu\nu)} = 3 \cdot \left(1 + \frac{\alpha_s}{\pi} + 5.2 \cdot \left(\frac{\alpha_s}{\pi} \right)^2 + \dots \right)$$

- relative number of 3-Jet events

$$R_3 = \frac{\sigma(e^+e^- \rightarrow 3\text{-Jets})}{\sigma(e^+e^- \rightarrow \text{Hadronen})} = C_1 \cdot \alpha_s + C_2 \cdot \alpha_s^2 + \dots$$

- distributions of event shape observables

$$\frac{d\sigma}{dO} = C_0 + C_1 \cdot \alpha_s + C_2 \cdot \alpha_s^2 + \dots$$

- in lepton-nucleon-scattering:

- scaling violations of structure functions

- jet rates and event shape observables

- sum rules

- from decays of heavy quarkonia

Update on World Summary of α_s

New Results since Summer 1998 [*S.B., hep-ex/9812026*]:

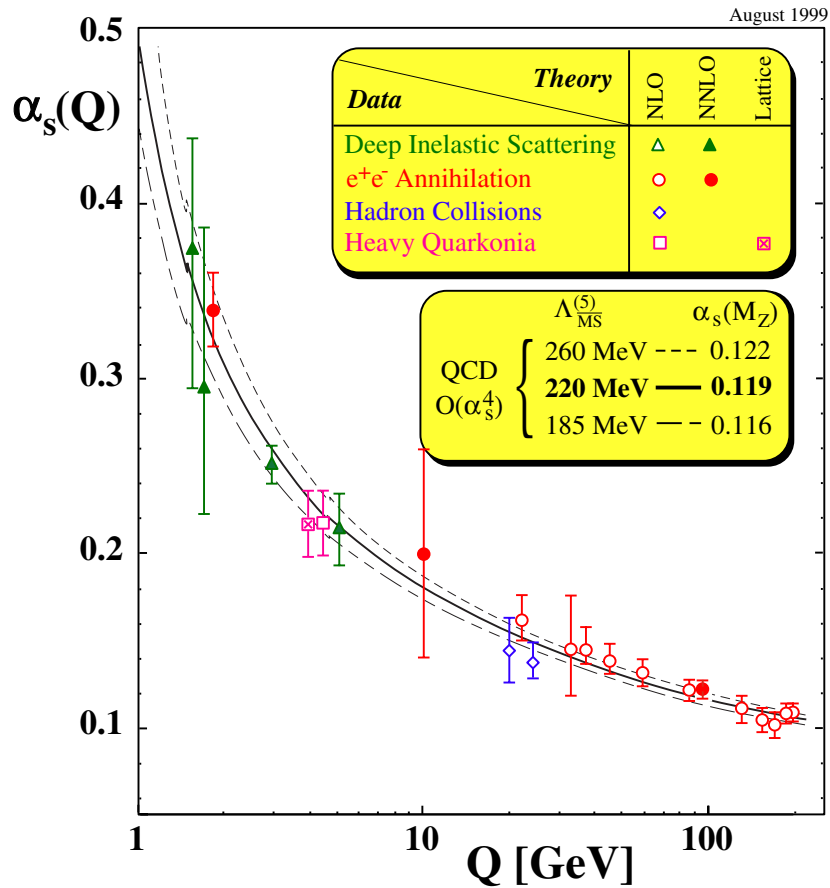
- α_s from xF_3 (**v-DIS**) in complete **NNLO** [*Kataev, Parente, Sidorov; hep-ph/9905310*]
- α_s from moments of F_2 (**μ -DIS**) in complete **NNLO** [*Santiago & Yndurain; hep-ph/9905310*]
- α_s from jet rates and event shapes at HERA: now combined
- α_s from Heavy Quarkonia and **Lattice Gauge Theory**: revised to smaller value and larger (5%) syst. uncertainty [*Spitz et al., hep-lat/9906009*]
- α_s from **Υ decays** [*Kühn, Penin and Pvoarov, hep-ph/9801356*]
- α_s from direct photon prod. in pp and p-pbar [*UA6, CERN-EP/99-21*]
- α_s from latest update of $\mathcal{R}_f = \Gamma(Z^0 \rightarrow \text{hadrons}) / \Gamma(Z^0 \rightarrow \mu^+\mu^-)$ [*J. Mnich, EPS99*]
- latest LEP results from hadronic **event shapes at LEP-2** [*M. Mangano, EPS99*]

Figure 34.

Process	Q [GeV]	$s(Q)$	$s(M_{Z^0})$	$s(M_{Z^0})$		Theory
				exp.	theor.	
<u>DIS [pol. struct. fctn.]</u>	0.7 - 8		0:120 + 0:010	+ 0:004	+ 0:009	NLO
DIS [Bj-SR]	1.58	0:375 + 0:062	0:121 + 0:008	0:005	0:006	NNLO
DIS [GLS-SR]	1.73	0:295 + 0:081	0:114 + 0:005	{	{	NNLO
-decays	1.78	0:339 + 0:092	0:121 + 0:009	+ 0:005	+ 0:009	NNLO
DIS [ν ; xF_3]	5.0	0:214 0:021	0:118 0:012	0:006	0:010	NNLO
DIS [e^- ; F_2]	2.96	0:252 0:021	0:1172 0:0024	0:001	0:003	NNLO
<u>DIS [e^-; jets & shps]</u>	7 - 100		0:118 0:006	0:002	0:006	NLO
<u>QQ states</u>	4.1	0:216 0:022	0:115 0:006	0:003	0:005	LGT
-decays	4.75	0:217 0:021	0:118 0:006	{	{	NLO
<u>e^+e^- [had]</u>	10.52	0:20 0:06	0:130 + 0:021	+ 0:021	{	NNLO
e^+e^- [jets & shaps]	22.0	0:161 + 0:016	0:124 + 0:029	0:005	+ 0:008	resum
e^+e^- [had]	34.0	0:146 + 0:011	0:123 + 0:009	+ 0:021	0:003	NLO
e^+e^- [jets & shaps]	35.0	0:145 + 0:031	0:123 + 0:021	0:002	+ 0:008	resum
e^+e^- [jets & shaps]	44.0	0:139 + 0:026	0:123 + 0:019	0:003	+ 0:005	resum
e^+e^- [jets & shaps]	58.0	0:132 + 0:012	0:123 + 0:008	0:003	+ 0:007	resum
pp ! bbX	20.0	0:145 + 0:007	0:113 0:006	+ 0:007	+ 0:008	NLO
<u>pp; pp ! X</u>	24.2	0:138 + 0:010	0:111 + 0:008	0:002	+ 0:009	NLO
(pp ! jets)	30 - 500	0:009	0:121 0:009	0:002	0:005	NLO
<u>e^+e^- [Z^0 ! had.]</u>	91.2	0:123 0:005	0:123 0:005	0:001	0:009	NNLO
e^+e^- [jets & shaps]	91.2	0:122 0:006	0:122 0:006	0:001	0:006	resum
e^+e^- [jets & shaps]	133.0	0:111 0:008	0:117 0:008	0:004	0:007	resum
e^+e^- [jets & shaps]	161.0	0:105 0:007	0:114 0:008	0:004	0:007	resum
e^+e^- [jets & shaps]	172.0	0:102 0:007	0:111 0:008	0:004	0:007	resum
e^+e^- [jets & shaps]	183.0	0:109 0:005	0:121 0:006	0:002	0:006	resum
e^+e^- [jets & shaps]	189.0	0:110 0:004	0:123 0:005	0:002	0:005	resum

TABLE 2. World summary of measurements of s . Underlined entries are new or updated since autumn 1998 (DIS = deep inelastic scattering; GLS-SR = Gross-Llewellyn-Smith sum rules; Bj-SR = Bjorken sum rules; (N)NLO = (next-to-)next-to-leading order perturbation theory; LGT = lattice gauge theory; resum. = resummed next-to-leading order).

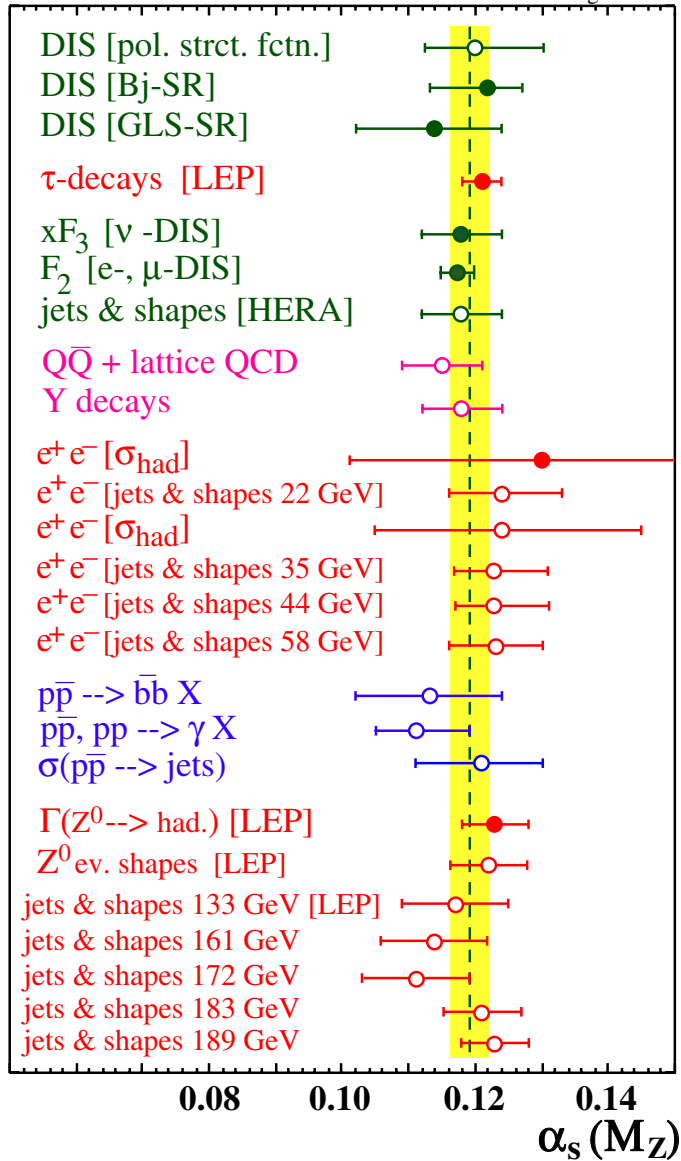
World Summary of $\alpha_s(Q)$



$$\alpha_s(M_Z) = 0.119 \pm 0.003 \iff \begin{cases} \Lambda_{\overline{\text{MS}}}^{(5)} = 220^{+40}_{-35} \text{ MeV} \\ \Lambda_{\overline{\text{MS}}}^{(4)} = 305^{+50}_{-45} \text{ MeV} \end{cases}$$

Figure 35.

August 1999



$$\alpha_s(M_Z) = 0.119 \pm 0.003$$

Figure 36.